High-spin states in the odd-odd nucleus ^{146}Tb

Krishichayan, A. Chakraborty, S. S. Ghugre, R. Goswami, S. Mukhopadhyay, N. S. Pattabiraman, S. Ray, and A. K. Sinha
Inter University Consortium For DAE Facilities, Calcutta Center, Sector III, LB-8, Bidhan Nagar, Kolkata 700 098, India

S. Sarkar
Department of Physics, The University of Burdwan, Burdwan 713 104, India

P. V. Madhusudhana Rao
Department of Nuclear Physics, Andhra University, Waltair 530 003, India

U. Garg
Department of Physics, University of Notre Dame, Notre Dame, Indiana 46556

S. K. Basu
Variable Energy Cyclotron Center, Sector-I/AF, Bidhan Nagar, Kolkata 700 064, India

B. K. Yogi
Department of Physics, Govt. College, Kota 324 009, India

L. Chaturvedi, A. Dhal, and R. K. Sinha
Department of Physics, Banaras Hindu University, Varanasi 221 005, India

M. Saha Sarkar and S. Saha
Saha Institute of Nuclear Physics, Sector-I/AF, Bidhan Nagar, Kolkata 700 064, India

R. Singh
Department of Physics and Astrophysics, University of Delhi, New Delhi 110 007, India

R. K. Bhowmik, A. Jhingan, N. Madhavan, S. Muralithar, S. Nath, R. P. Singh, and P. Sugathan
Nuclear Science Center, Aruna Asaf Ali Marg, New Delhi 110 067, India
(Received 8 June 2004; published 26 October 2004)

The odd-odd ^{146}Tb nucleus has been investigated using the ^{115}In(^{34}S,$3n$) reaction at 140 MeV incident energy using an array of eight Compton-suppressed Clover detectors. Based on the observed γ-γ coincidences, the level structure of ^{146}Tb has been extended up to $E_x \sim 10$ MeV. Linear polarization measurements have been combined with angular correlations of the observed γ rays to assign the electromagnetic nature to the transitions. Probable origin of a cascade of $M1$ transitions observed around 8 MeV excitation energy has been discussed.

DOI: 10.1103/PhysRevC.70.044315 PACS number(s): 27.60.+j, 23.20.Lv, 23.20.En, 21.60.Cs

I. INTRODUCTION

Nuclei close to the doubly closed ^{146}Gd have drawn considerable attention, both experimentally and theoretically, due to their proximity to the $N=82$ and $Z=64$ shell closure. The excitation spectra in the low-energy region for these nuclei show irregular and complex patterns, typical for near-spherical nuclei and are dominated by single- and multiparticle excitations. Spectroscopic information on these levels provides important avenues to the empirical single particle energies and the residual N-N interactions needed for understanding nuclear structure in the shell model framework. With increasing excitation energies and angular momenta, a certain regularity develops in their spectra due to various underlying reasons. For example, they show collective bands with moderate deformations, as well as superdeformation [1]. Moreover, due to availability of particles and holes in high-j orbitals, such as $\pi h_{11/2}^{n}$ and $\nu h_{11/2}^{-n}$, phenomena like magnetic rotation could be expected, and have, in fact, been observed in nearby ^{142,143,144}Gd [2,3], ^{141,144}Eu [4,5] nuclei.

The odd-odd ^{146}Tb nucleus, with 65 protons and 81 neutrons, has been studied earlier both experimentally and theoretically and it has been found that the low-lying excitation spectra up to $\sim 4-5$ MeV and $J \sim 20\hbar$ are irregular, originating primarily from single- and multiparticle excitations. Collatz *et al.* [6] performed two in-beam experiments, using ^{7}Li and ^{31}P beams and modest γ-detector arrays, and proposed a level scheme up to around 5 MeV excitation and $19\hbar$ spin. The authors suggested that the observed states up to $J^{\pi} = 19^{-}$ spin can be identified with $4qp$ excitations involving an $h_{11/2}$ proton particle and an $h_{11/2}$ neutron hole, coupled to the proton particle-hole yrast excitations in ^{146}Gd. The present work was initiated with the motivation to extend the level

scheme to higher spins and the preliminary results from this investigation were presented earlier [7]. After our work was completed, we came across a report by Xie *et al.* [8]. They have used ^{118}Sn(^{32}S, $1p3n$) reaction at 165 MeV, and have presented the level scheme up to about 8.4 MeV, built on the 1.18 ms isomeric 10^+ level with $(\pi h_{11/2} \nu h_{11/2}^{-1})$ configuration and alluded to the possibility of core excitations. However, they were unable to make unambiguous spin-parity assignments to many of the levels. In our work, the level scheme of ^{146}Tb has been extended up to higher excitation energies, and a new feature, a sequence of levels above ~8 MeV, connected by $M1$ transitions has been observed. In addition, the use of the Clover detector array has permitted polarization measurements, which, coupled with the γ-ray angular correlation measurements, have helped assign uniquely the spins and parities in the observed level structure.

II. EXPERIMENTAL PROCEDURE AND RESULTS

The reaction ^{115}In(^{34}S, $3n$) at a beam energy of 140 MeV was used in order to populate high-spin states in ^{146}Tb. γ-γ coincidence measurements, using a target of ~1.29 mg/cm^2 enriched ^{115}In with a ~7.14 mg/cm^2 Au backing, were performed with the Indian National Gamma Array (INGA), stationed at the 15UD Pelletron facility at Nuclear Science Centre (NSC), New Delhi. For this experiment, the INGA comprised of eight Compton-suppressed Clover detectors. The efficiency for a Clover detector (after add-back), used in the array is typically around 0.17% (photopeak) at ~1 MeV [9]. These detectors were placed at 80° and 140° with respect to the beam direction. A total of about 220 million two- or higher-fold γ-γ coincidence events were recorded in the experiment. After accurate gain-matching and requisite corrections for any on-line drifts [10], the coincidence events were sorted into symmetric and asymmetric (angle dependent) matrices for detailed off-line analysis. The data were analyzed using both RADWARE [11] and IUCSORT [10,12] analysis packages.

The level scheme of ^{146}Tb has been established up to E_x ~10.6 MeV in excitation energy and a tentative spin of J ~30$\hbar$ (Fig. 1). In addition to the transitions reported by Xie *et al.* [8], about 15 new transitions have been identified in the present work. These transitions are indicated by asterisk in the level scheme. Representative background-subtracted gated spectra associated with three sequences (sequence I, II, and III) are shown in Figs. 2, 3, and 4.

Multipolarity of the de-exciting γ rays from ^{146}Tb were deduced from the observed γ ray angular correlations [13,14]. For $R_{\rm DCO}$, the coincidence data were sorted into an asymmetric matrix whose one axis corresponded to γ ray energy deposited in the detectors at 140° while the other axis corresponded to the γ ray energy deposited in the detectors at 80°. A gate corresponding to a γ ray of known multipolarity was made on one axis (say, the x axis) and the coincidence spectrum was projected on the other axis (y axis). Next the same gate was set on the y axis and projection was made on the x axis. Assuming stretched transitions, the intensities of the transitions which had the same multipolarity as the gated γ ray were approximately the same in both the spectra. If the γ rays were of different multipolarity, the intensities differed by a factor of almost 2. Using sum gates of known dipole transitions, we define $R_{\rm DCO}$ as

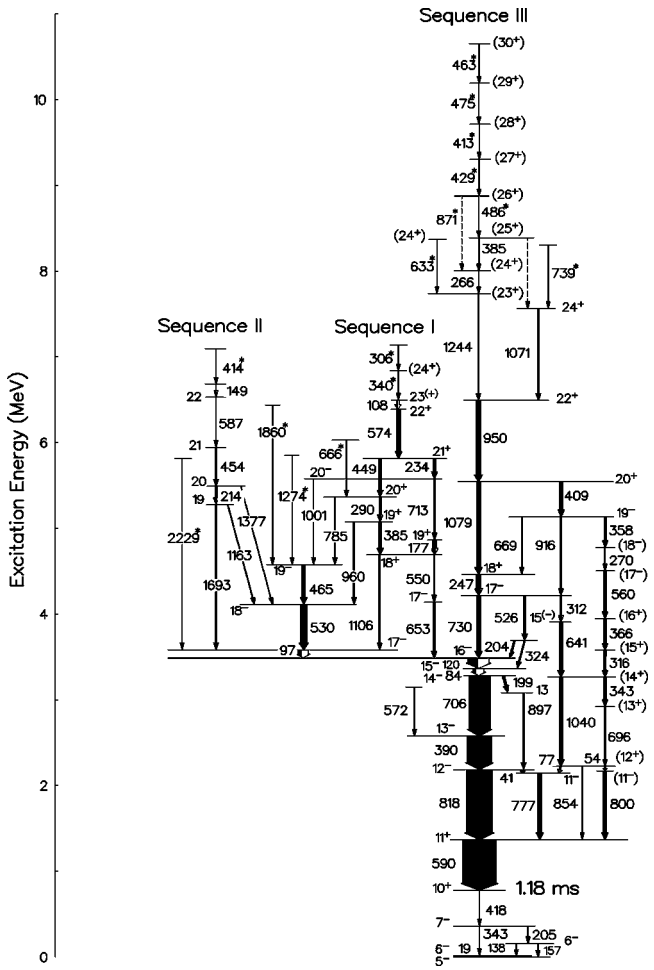

FIG. 1. The level scheme of ^{146}Tb for the levels populated in ^{115}In(^{34}S, $3n$) reaction. The width of the arrows approximately represents the observed intensities. The transitions marked with asterisk are in addition to those reported in Refs. [7] and [8].

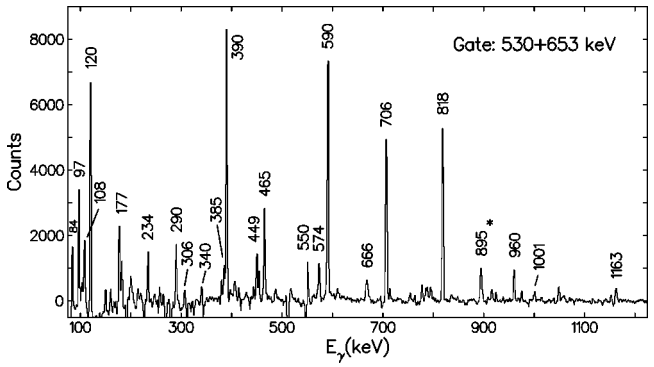

FIG. 2. Representative γ-γ coincidence spectrum with simultaneous gates on the 530 and 653 keV transitions of sequence I. The transition marked with asterisk belong to neighboring nuclei.

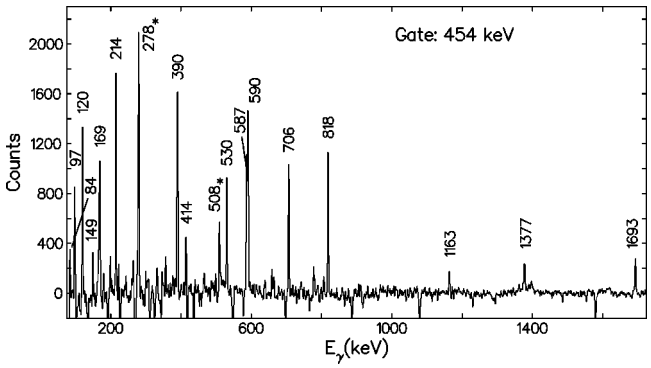

FIG. 3. γ-γ coincidence spectrum for sequence II. The transitions marked with asterisk belong to neighboring nuclei.

$$R_{\mathrm{DCO}} = \frac{I_{\gamma_1}\ at\ 80^\circ\ ,\ gated\ with\ \gamma_2\ at\ 140^\circ}{I_{\gamma_1}\ at\ 140^\circ\ ,\ gated\ with\ \gamma_2\ at\ 80^\circ}.$$

The observed values of R_{DCO} are illustrated in Fig. 5 and detailed results are given in Table I. The R_{DCO} value for known dipole transitions is $\sim$1.1 and is 1.8 for known quadrupoles, using gate on dipole transitions. These values were cross checked for self-consistency. Further, they reproduced the results for the known multipolarities [$\Delta J=1$ and $\Delta J=2$] in the neighboring nuclei.

The use of Clover detectors facilitated polarization measurements [15–17]. These measurements, even though qualitative, were crucial for assignment of the parities in the observed level structure. The linear polarization of the radiation can typically be determined through a difference between the number of Compton scattered γ rays in the reaction plane $N_{\|}$, and perpendicular to it, $N_{\perp}$.

As an example of this data, Fig. 6 shows the background subtracted perpendicular and parallel coincidence spectra (with respect to the beam direction) for 413, 463, 475, and 486 keV γ ray transitions. All these γ rays indicate a preferential scattering in parallel direction, which is a characteristic of magnetic transitions. Coupled with the results of angular correlations (Fig. 5), these transitions have been assigned $M1$

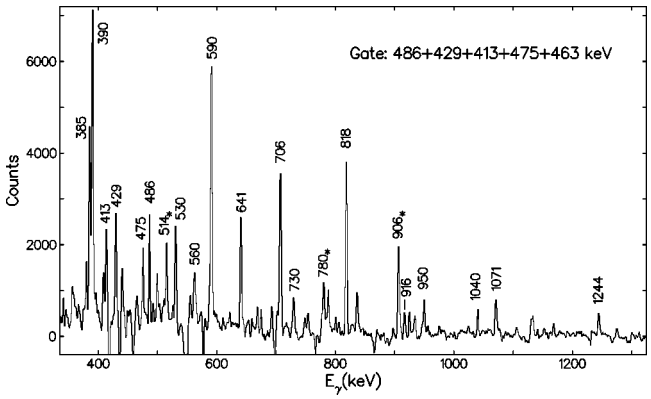

FIG. 4. Part of the γ spectrum obtained from the sum gate of 413, 429, 463, 475, and 486 keV transitions (members of $M1$ sequence), to indicate their placement. The transitions marked with asterisk belong to neighboring nuclei.

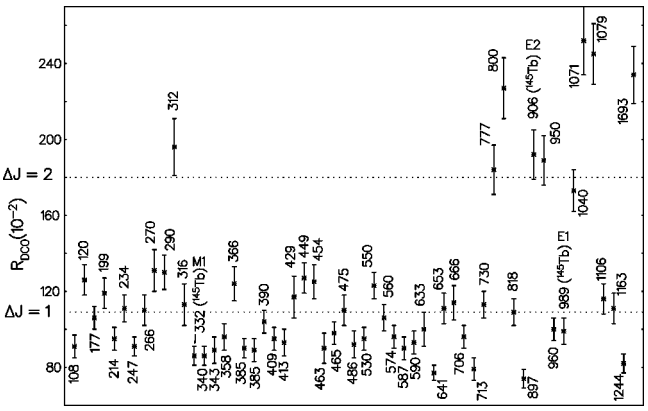

FIG. 5. γ ray anisotropy intensity ratio R_{DCO}, for the transitions belonging to ^{146}Tb. The lines correspond to the values obtained for known dipole and quadrupole transitions using sum of stretched dipoles and have been drawn to guide the eye. The quoted error includes error due to background subtraction, peak fitting, and effieciency correction. For comparison, few transitions belonging to ^{145}Tb are also shown.

multipolarity. The right part of Fig. 6 indicates that the 950, 1079, and 1106 keV γ rays are electric in nature whereas the 1244 keV γ ray is magnetic.

A polarization matrix was constructed from the data corresponded to energy recorded in any detector on one axis, while the other axis corresponded to the energy scattered in a perpendicular or parallel segment of the Clover with respect to the beam axis. From the projected spectra, the number of perpendicular ($N_{\perp}$) and parallel ($N_{\|}$) scatters for a given γ ray could be obtained. From these spectra the asymmetry parameter Δ_{IPDCO} was obtained using the relation

$$\Delta_{\mathrm{IPDCO}} = \frac{[a(E_\gamma)N_{\perp}] - N_{\|}}{[a(E_\gamma)N_{\perp}] + N_{\|}}.$$

The correction parameter a due to the asymmetry of the present experimental configuration has been deduced from radioactive sources, and is a function of the γ ray energy, i.e.,

$$a(E_\gamma) = a_0 + a_1 E_\gamma,$$

where, $a_0 = 1.016(6)$ and $a_1 = -1.32(53) \times 10^{-5}$. A near zero value for Δ_{IPDCO} is indicative of admixture, whereas a pure electric or magnetic transition results in a positive and negative value, respectively, for the Δ_{IPDCO}. These results are listed in Table I and, coupled with our angular correlation data, form the basis of assignments of the multipolarity of the observed transitions.

Figure 7 illustrates a two-dimensional plot of asymmetry parameter Δ_{IPDCO} versus angular correlation R_{DCO}, as defined earlier. As seen from the plot, the polarization and multipolarity measurements together can give us a reasonable assignment of the spin and parity for the levels without recourse to detailed theoretical calculations.

The polarization data necessitated some changes in the previously reported spin-parity assignments for few levels. Collatz *et al.* [6] had assigned $E1$ nature for the 730 keV transition de-exciting the 4.218 MeV level in the yrast se-

TABLE I. Gamma transition energy (E_γ) in keV, excitation energy (E_x) in keV, initial and final spins for the transition, relative intensity (I_γ), DCO and IPDCO ratio for the γ ray transitions in ^{146}Tb. Unless otherwise mentioned, the values in column 5 are obtained from sum gate of 590, 818, 390, and 760 keV dipole transitions.

E_γ	E_x	$J_i^\pi \rightarrow J_f^\pi$	I_γ[a]	R_{DCO}	Δ_{IPDCO}
83.7	3368.2	$15^- \rightarrow 14^-$	9.2(1.0)		
97.0	3585.1	$17^- \rightarrow 16^-$	11.4(1.5)		
107.9	6495.7	$23^{(+)} \rightarrow 22^+$	3.9(0.4)	0.91(0.06)	
119.9	3488.1	$16^- \rightarrow 15^-$	34.4(4.0)	1.26(0.08)	
149.3	6683.9		*W*[b]		
177.1	4867.7	$19^+ \rightarrow 18^+$	10.0(1.1)	1.06(0.06)	−0.04(0.05)
199.4	3285.1	$14^- \rightarrow 13$	6.2(0.7)	1.19(0.08)[c]	
203.7	3691.8		4.4(0.6)		
214.4	5492.4	$20 \rightarrow 19$	5.6(0.6)	0.95(0.06)	
233.7	5814.2	$21^+ \rightarrow 20^-$	8.7(1.0)	1.11(0.07)	
247.3	4465.0	$18^+ \rightarrow 17^-$	15.1(1.7)	0.91(0.05)	0.08(0.05)
266.5	8004.0	$(24^+) \rightarrow (23^+)$	1.1(0.2)	1.10(0.08)	
269.7	4775.9	$(18^-) \rightarrow (17^-)$	*W*[b]	1.31(0.11)[c]	
289.9	5365.1	$20^+ \rightarrow 19^+$	7.1(0.7)	1.30(0.09)	−0.03(0.02)
306.5	7593.0		*W*[b]		
312.3	4217.8	$17^- \rightarrow 15^{(-)}$	4.2(0.7)	1.96(0.15)[c]	0.13(0.07)
316.0	3580.0	$(15^+) \rightarrow (14^+)$	6.3(1.0)	1.13(0.11)[c]	−0.06(0.04)
323.8	3692.0		3.5(0.4)		
340.4	6836.1	$(24^+) \rightarrow 23^{(+)}$	*W*[b]	0.86(0.05)	
343.2	3264.0	$(14^+) \rightarrow (13^+)$	6.3(1.0)	0.89(0.07)[c]	−0.06(0.06)
358.3	5134.3	$19^- \rightarrow (18^-)$	5.8(0.7)	0.96(0.07)[c]	−0.07(0.05)
365.7	3945.7	$(16^+) \rightarrow (15^+)$	7.3(1.1)	1.24(0.09)[c]	0.02(0.03)
384.9	5075.7	$19^+ \rightarrow 18^+$	11.1(1.5)	0.90(0.05)	−0.02(0.03)
385.2	8389.2	$(25^+) \rightarrow (24^+)$	2.3(0.4)	0.89(0.06)	
389.6	2578.1	$13^- \rightarrow 12^-$	90.0(10.5)	1.04(0.06)	−0.02(0.01)
408.8	5543.1	$20^+ \rightarrow 19^-$	10.2(1.1)	0.95(0.06)	0.10(0.05)
413.4	9717.9	$(28^+) \rightarrow (27^+)$	0.7(0.1)	0.93(0.07)	
414.1	7098.0		*W*[b]		
429.3	9304.5	$(27^+) \rightarrow (26^+)$	0.7(0.1)	1.17(0.11)	
449.5	5814.3	$21^+ \rightarrow 20^+$	9.1(1.1)	1.27(0.08)	−0.17(0.03)
453.9	5947.3	$21 \rightarrow 20$	5.6(0.6)	1.25(0.09)	
463.1	10 655.5	$(30^+) \rightarrow (29^+)$	*W*[b]	0.90(0.08)	
464.7	4579.9	$19^- \rightarrow 18^-$	12.2(1.5)	0.98(0.06)	−0.02(0.01)
474.6	10 192.4	$(29^+) \rightarrow (28^+)$	0.4(0.1)	1.10(0.08)	
486.0	8875.2	$(26^+) \rightarrow (25^+)$	1.2(0.3)	0.92(0.07)	−0.07(0.03)
525.7	4217.7		8.5(1.0)		
530.1	4115.2	$18^- \rightarrow 17^-$	22.6(2.6)	0.95(0.06)	−0.03(0.02)
549.8	4690.6	$18^+ \rightarrow 17^-$	3.2(0.6)	1.23(0.07)	0.08(0.06)
560.5	4506.2	$(17^-) \rightarrow (16^+)$	7.0(1.1)	1.06(0.07)[c]	0.05(0.04)
572.0	2760.6		2.7(0.5)		
573.6	6387.8	$22^+ \rightarrow 21^+$	12.0(1.7)	0.96(0.06)	−0.08(0.05)
587.3	6534.6	$22 \rightarrow 21$	*W*[b]	0.90(0.06)	
590.5	1370.5	$11^+ \rightarrow 10^+$	>125	0.93(0.06)	−0.02(0.01)
633.0	8370.5	$(24^+) \rightarrow (23^+)$	0.5(0.1)	1.00(0.09)	
640.6	3905.5	$15^{(-)} \rightarrow (14^+)$	11.2(1.8)	0.77(0.04)[c]	0.14(0.07)
652.7	4140.8	$17^- \rightarrow 16^-$	7.0(0.7)	1.11(0.08)	−0.07(0.04)

TABLE I. (*Continued.*)

E_γ	E_x	$J_i^\pi \rightarrow J_f^\pi$	I_γ[a]	R_{DCO}	Δ_{IPDCO}
666.4	5742.1		3.2(0.4)	1.14(0.09)	
669.5	5134.6	$19^- \rightarrow 18^+$	2.7(0.4)		
696.3	2920.8	$(13^+) \rightarrow (12^+)$	2.5(0.5)		
706.4	3284.5	$14^- \rightarrow 13^-$	80.9(9.3)	0.96(0.06)	−0.02(0.01)
713.3	5581.0	$20^- \rightarrow 19^+$	3.3(0.4)	0.79(0.06)	0.04(0.03)
729.6	4217.7	$17^- \rightarrow 16^-$	14.9(1.7)	1.13(0.07)	−0.03(0.02)
739.1	8302.8		*W*[b]		
777.4	2147.9	$11^- \rightarrow 11^+$	15.0(2.4)	1.84(0.13)[c]	0.03(0.02)
785.0	5364.9	$20^+ \rightarrow 19^-$	3.7(0.4)		
800.5	2171.0	$(11^-) \rightarrow 11^+$	11.2(1.8)	2.27(0.16)[c]	0.02(0.03)
818.1	2188.6	$12^- \rightarrow 11^+$	100	1.09(0.07)	0.02(0.01)
854.1	2224.6	$(12^+) \rightarrow 11^+$	1.1(0.3)		
870.6	8875.2	$(26^+) \rightarrow (24^+)$	*W*[b]		
896.9	3085.7	$13 \rightarrow 12^-$	5.6(1.0)	0.74(0.05)[c]	
916.4	5134.1	$19^- \rightarrow 17^-$	4.8(0.6)		
949.6	6493.0	$22^+ \rightarrow 20^+$	17.4(2.1)	1.89(0.13)	0.08(0.03)
960.0	5075.2	$19^+ \rightarrow 18^-$	5.0(0.6)	1.00(0.06)	0.05(0.03)
1000.6	5580.5	$20^- \rightarrow 19^-$	*W*[b]		
1040.3	3264.9	$(14^+) \rightarrow (12^+)$	12.2(1.8)	1.73(0.11)[c]	0.02(0.02)
1070.7	7563.7	$24^+ \rightarrow 22^+$	4.6(0.6)	2.52(0.18)	0.23(0.12)
1078.6	5543.5	$20^+ \rightarrow 18^+$	14.9(1.7)	2.45(0.16)	0.09(0.04)
1105.7	4690.8	$18^+ \rightarrow 17^-$	4.8(0.6)	1.16(0.08)	
1162.6	5277.6	$19 \rightarrow 18^-$	2.3(0.2)	1.11(0.08)	
1244.5	7737.5	$(23^+) \rightarrow 22^+$	4.4(0.6)	0.82(0.05)	
1273.8	5853.7		*W*[b]		
1377.4	5492.6	$20 \rightarrow 18^-$	1.6(0.4)		
1692.9	5278.0	$19 \rightarrow 17^-$	5.4(0.6)	2.34(0.15)	
1860.0	6439.9		*W*[b]		
2229.0	5811.1		*W*[b]		

[a]The quoted errors on intensities encompass errors due to background subtraction, peak fitting and efficiency correction.
[b]*W* indicates weak transitions whose intensity could not be computed.
[c]R_{DCO} from gate on 590 keV dipole transition.

quence. The polarization results (Fig. 7) indicate a "magnetic" nature for this transition. Hence, we have assigned it firmly as $M1$ transition. Based on this assignment, the spin parity of the levels in this sequence up to 22^+ have been established. The 800 keV transition originating from the level at E_x=2.171 MeV was assigned as $E1$ (with $\Delta J=-1$) by the earlier groups [6,8]. As seen in Fig. 7, this transition is, indeed, electric in nature. Assuming the earlier assignment of $\Delta J=-1$ for this transition, we should have obtained a value of $R_{\mathrm{DCO}} \sim 1$. The R_{DCO} value for this transition is $\sim$2.2, which could correspond to either $\Delta J=0$ or $\Delta J=2$ change in angular momentum. Hence, the $\Delta J=-1$ assignment is ruled out. The present experiment has helped us unambiguously assign a spin parity of $J^\pi=19^-$ to the level at E_x=5.134 MeV. The spin-parity assignments for the subsequent low-lying levels indicate $J^\pi=12^+$ for the level at E_x =2.225 MeV. The observation of parallel decay paths and crossover transitions, above the level at E_x=2.225 MeV confirm this $J^\pi=12^+$ assignment. This level de-excites via the 54 keV transition to the E_x=2.171 MeV. Assuming the earlier assignment of $J^\pi=10^-$ for this level (i.e., $\Delta J=-1$ nature for the 800 keV transition) would demand a $M2$ multipolarity for the 54 keV transition. This would correspond to a μs lifetime, which is not within our coincidence time window. Since the 696, 343, and 1040 keV and other above transitions are observed in coincidence with the 800 keV transition, the $M2$ multipolarity for the 54 keV transition is not possible. This supports the tentative assignment of $J^\pi=11^-$ for the level at E_x=2.171 MeV which de-excites via the 800 keV transition. A point worth mentioning is that in ^{145}Tb, a neighboring nucleus which was populated in a similar reaction [18], the 514 keV γ transition de-exciting the $J^\pi=15/2^+$

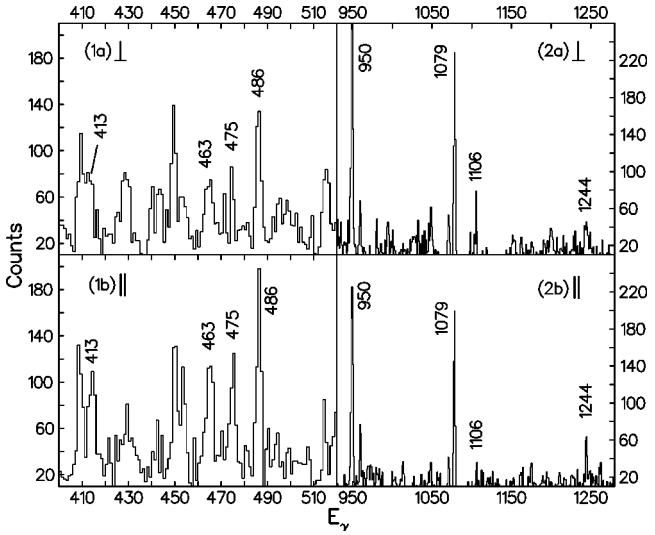

FIG. 6. Background subtracted perpendicular and parallel coincidence spectra (with respect to the beam direction) for the 413, 463, 475, 486, 950, 1079, 1106, and 1244 keV transitions.

level at 1.420 MeV was assigned on the basis of a ratio of the angular distribution taken at two angles (see Ref. [18] for more details). This measured ratio, 1.45(25), could be interpeted as a stretched quadrupole which is expected to have a ratio of 1.4, but it is also very similar to the value for transitions involving no spin change. The authors had assigned this transition as a $\Delta J=0$, electric transition [18]. Further, in ^{146}Tb, Collatz *et al.* [6] and Xie *et al.* [8] had assigned a $\Delta J=0$ change in angular momentum for the 777 keV transition, which is electric in nature. Both the 800 and 777 keV transitions de-excite to the same level ($E_x=1.370$ MeV). Hence, the 800 keV transition is tentatively assigned as a $\Delta J=0$, electric transition. Thus, the level at $E_x=2.171$ MeV

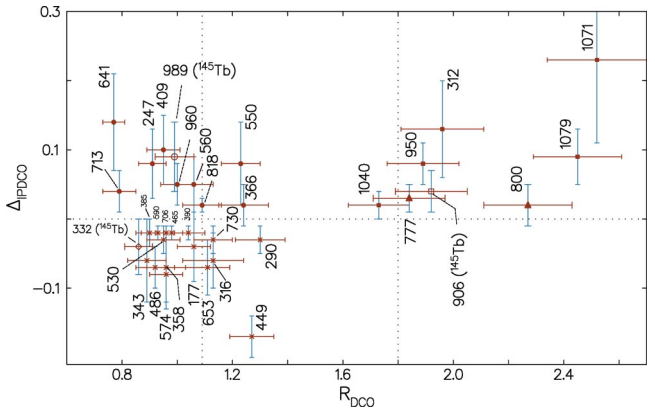

FIG. 7. (Color online) Two-dimentional plot of the asymmetry parameter Δ_{IPDCO} vs the angular correlation ratio R_{DCO}. Filled circles denote $E1$ transitions, filled squares $E2$ transitions, asterisks $M1$ transitions, and filled upwards-pointing triangles $\Delta J=0$ transitions. For comparison few transitions belonging to ^{145}Tb are also shown. The dotted lines parallel to the y axis correspond to the value obtained for known dipole and quadrupole transitions. The dotted line parallel to the x axis indicates the zero value of Δ_{IPDCO}. These lines have been drawn to guide the eye.

is now assigned as $J^\pi=11^-$ and the level at 2.225 MeV is assigned as $J^\pi=12^+$, assuming $E1$ multipolarity for both the 54 and 77 keV transitions. The 366 keV transition involves a change in angular momentum of $\Delta J=1$ unit, as seen in Fig. 5. This contradicts the earlier assignment of $\Delta J=2$ nature of this transition [8]. The polarization measurements indicate a mixed nature, and hence the 366 keV transition is tentatively assigned as $M1/E2$, and the multipolarity of the level at $E_x=3.946$ MeV is $J^\pi=16^+$. The present measurements are indicative of a $M1$ nature for the 358 keV transition ($E_x=5.135$ MeV); it was earlier reported as a $\Delta J=0$ transition.

The observed transitions belonging to ^{146}Tb are summarized in Table I. In addition to the γ transitions reported by Xie *et al.* [8], we have observed the following γ transitions (energies in keV): 306, 340($M1$), 413($M1$), 414, 429($M1$), 463($M1$), 475($M1$), 486($M1$), 633($M1$), 666, 739, 871($E2$), 1274, 1860, and 2229. The spin and parity of the levels depopulating via the 306, 414, 666, 739, 1274, 1860, and the 2229 keV transitions could not be ascertained from the present data. We have not observed the 558 and 272 keV transitions, de-exciting the level at $E_x=4.777$ and 4.218 MeV, respectively, reported in the earlier investigation [8].

As seen from the Fig. 1, the absence of any pronounced band like structure, is indicative of persistence of single particle behavior in this nucleus. The presence of high energy transitions and fragmentation of intensity into several cascades are indicative of excitation of nucleons across the shell gaps.

III. DISCUSSION

The low-lying excitation spectra of ^{146}Tb up to $E_x\sim4.5$ MeV have been interpreted within the shell model framework [6,8,19,20]. The states up to $E_x\sim1.5$ MeV originate primarily due to the coupling of one proton-particle with one neutron-hole outside the ^{146}Gd core. The ground state has spin-parity 5^- and is thought to arise from an admixture of $\pi h_{11/2}\nu s_{1/2}^{-1}$ and $\pi h_{11/2}\nu d_{3/2}^{-1}$ configurations. The levels above the 11^+ state of the $(\pi h_{11/2}\nu h_{11/2}^{-1})$ multiplet at $E_x\sim1.5$ MeV involve the ^{146}Gd core excitation [6,8]. The multiplet of negative-parity states of $(\pi h_{11/2}\nu h_{11/2}^{-1})\otimes3^-$ character are observed around 2 MeV energy of excitation, whereas the states around $E_x\sim3.2$ MeV, multiplets arise from the $(\pi h_{11/2}\nu h_{11/2}^{-1})\otimes2^+$ and $(\pi h_{11/2}\nu h_{11/2}^{-1})\otimes4^+$ coupling: the $3^-,2^+,4^+$ bosons are from the ^{146}Gd core excitations [6,8]. The $Z=64$ proton shell closure is much weaker than the $N=82$ neutron shell closure. Hence, the proton core excitation is energetically favored at comparatively lower excitation energies.

We have tried here to interpret, qualitatively, the observed levels considering the shell model valence space obtained from experimental low-lying spectra of one neutron-particle $^{147}_{64}$Gd$_{83}$, one neutron-hole $^{145}_{64}$Gd$_{81}$, one proton-particle $^{147}_{65}$Tb$_{82}$ and one proton-hole $^{145}_{63}$Eu$_{82}$ with respect to ^{146}Gd core [21]. The valence space considered consists of $\pi(1g_{7/2},2d_{5/2},1h_{11/2},3s_{1/2},2d_{3/2})$ and the $\nu(1g_{7/2},2d_{5/2},1h_{11/2},2d_{3/2},3s_{1/2},2f_{7/2},1i_{13/2})$ orbitals.

The possible configurations for the observed level structure are listed in Table II. The approximate energy ranges for

TABLE II. Probable shell model configurations of the observed levels in ^{146}Tb.

Configuration	J^{π}[a]	Energy (MeV) domain in the expt. spectra.
$\pi h_{11/2}\nu s_{1/2}^{-1}$	$6^-, 5^-, \ldots$	
$\pi h_{11/2}\nu d_{3/2}^{-1}$	$7^-, 6^-, \ldots$	$\sim$0.4
$\pi h_{11/2}\nu h_{11/2}^{-1}$	$11^+, 10^+, \ldots$	$\sim$1.5
$(\pi h_{11/2}\nu h_{11/2}^{-1})\otimes 3^-$	$13^-, 12^-, \ldots$	$\sim$2.1–2.5
$\pi h_{11/2}s_{1/2}d_{5/2}^{-1}\nu h_{11/2}^{-1}$	$14^+, 13^+, \ldots$	
$\pi h_{11/2}d_{3/2}d_{5/2}^{-1}\nu h_{11/2}^{-1}$	$15^+, 14^+, \ldots$	$\sim$2.2–3.5
$\pi h_{11/2}^2 d_{5/2}^{-1}\nu h_{11/2}^{-1}$	$18^-, 17^-, \ldots$	
$\pi h_{11/2}^2 g_{7/2}^{-1}\nu h_{11/2}^{-1}$	$19^-, 18^-, \ldots$	
$\pi h_{11/2}^3 d_{5/2}^{-2}\nu s_{1/2}^{-1}$	$18^-, 17^-, \ldots$	
$\pi h_{11/2}^3 d_{5/2}^{-2}\nu d_{3/2}^{-1}$	$19^-, 18^-, \ldots$	
$\pi h_{11/2}^3 g_{7/2}^{-2}\nu s_{1/2}^{-1}$	$20^-, 19^-, \ldots$	
$\pi h_{11/2}^3 g_{7/2}^{-2}\nu d_{3/2}^{-1}$	$21^-, 20^-, \ldots$	$\sim$3.2–5.5
$\pi h_{11/2}^3 d_{5/2}^{-2}\nu h_{11/2}^{-1}$	$23^+, 22^+, \ldots$	
$\pi h_{11/2}^3 g_{7/2}^{-2}\nu h_{11/2}^{-1}$	$25^+, 24^+, \ldots$	$\sim$4.4–6.8
$\pi h_{11/2}\nu h_{11/2}^{-3} f_{7/2}^2$	$25^+, 24^+, \ldots$	$\sim$5.2–7.0
$\pi h_{11/2}^3 d_{5/2}^{-2}\nu h_{11/2}^{-3} f_{7/2}^2$	$37^+, 36^+, \ldots$	$\sim$7.7–10.6
$\pi h_{11/2}^3 g_{7/2}^{-2}\nu h_{11/2}^{-3} f_{7/2}^2$	$39^+, 38^+, \ldots$	

[a]The value corresponds to first two maximum aligned spins that could be obtained for the given configuration.

different configurations mentioned in Table II are based on the observation of experimental levels predominantly belonging to these configurations. For convenience of discussion, the proposed level scheme has been labeled in three sequences above the excitation energy of $\sim$4 MeV. The positive parity states of sequence I are likely result from configurations such as $\pi h_{11/2}^3 d_{5/2}^{-2}\nu h_{11/2}^{-1}$ and $\pi h_{11/2}^3 g_{7/2}^{-2}\nu h_{11/2}^{-1}$. These configurations result in a maximum aligned spin of $J^{\pi}=23^+$ and 25^+, respectively. Hence, the levels of this sequence starting from 18^+ at $\sim$4.7 MeV may be due to proton excitation from ^{146}Gd core. Possible configurations for the negative parity states are also given in Table II. At relatively higher excitation energy, $E_x>5$ MeV, one may observe states involving neutron excitation across $N=82$ shell closure, as indicated also by Xie *et al.* [8]. Sequence II can then be attributed to the neutron core breaking, which is supported by the presence of very high energy γ transitions. The levels of sequence II may be arising from the configuration $\pi h_{11/2}\nu h_{11/2}^{-3} f_{7/2}^2$.

Sequence III is most interesting in the present work, and consists of a "band" between spins 23^+ and 30^+ with somewhat irregular level spacings. These levels are connected by $\Delta J=1$ stretched magnetic transitions; only one very weak crossover $E2$ transition has been observed.

Similar $\Delta J=1$ cascades have also been observed in ^{143,144,145}Tb [18,22,23] nuclei at different excitation energies. In ^{143,145}Tb, a $\Delta J=1$ cascade has been observed at around $E_x\sim 5$ MeV, whereas in ^{144}Tb such a cascade has been observed at a relatively lower excitation energy ($E_x\sim 2.6$ MeV). In ^{143}Tb, this cascade has been confirmed as an $M1$ band [22]. The present $M1$ transition cascade (sequence III) in ^{146}Tb is found at a relatively higher excitation energy ($E_x\sim 8$ MeV). This sequence de-excites through the high energy γ rays (1244,950,1079 keV) similar to that in ^{144}Tb (955,1306,1377 keV) [23]. A number of $\Delta J=1$ ($M1$) bands in the neighboring $^{142-144}$Gd [2,3], ^{141}Eu [4] nuclei have been identified as "shears" bands. Weak deformation and existence of high-j particles of one kind of nucleons and high-j holes of other kind give rise to the formation of "shears" band in this mass region [24]. Although the energy spacings of these magnetic rotational bands in ^{142}Gd and ^{141}Eu are regular and follow the $I(I+1)$ law, the level spacings of the magnetic band are irregular in ^{144}Gd [2,3] which is closer to ^{146}Gd. Such irregular magnetic bands have also been seen in ^{143}Gd [2,3] and in ^{194,197}Pb [25].

The level spacings of sequence III also do not follow the $I(I+1)$ law. As pointed out earlier, two sequences (sequence I and sequence II), probably built on high-j proton particles $\pi(h_{11/2}^3 d_{5/2}^{-2})\nu(h_{11/2}^{-1})$ and high-j neutron holes $\pi(h_{11/2})\nu(h_{11/2}^{-3} f_{7/2}^2)$, have been observed at $\sim$4.7 and $\sim$5.2 MeV, respectively. So, one may expect to observe a sequence of levels from the multiplet built on $(\pi h_{11/2}^3 d_{5/2}^{-2})\otimes(\nu h_{11/2}^{-3} f_{7/2}^2)$ configuration at around 10 MeV of excitation energy. Each of these proton and neutron configurations can contribute nearly same angular momentum values and may form two blades of shears. Sequence III, at $E_x\sim 8$ MeV, resembles a shears band with $(\pi h_{11/2}^3 d_{5/2}^{-2})\otimes(\nu h_{11/2}^{-3} f_{7/2}^2)$ configuration and the irregular nature may be due to its closeness to ^{146}Gd core. As already discussed, that sequence I might have its origin in either $(\pi h_{11/2}^3 d_{5/2}^{-2}\nu h_{11/2}^{-1})$ or $(\pi h_{11/2}^3 g_{7/2}^{-2}\nu h_{11/2}^{-1})$ configuration, or in both, and the configuration mixing may give rise to the observed irregularity.

IV. CONCLUSION

The level scheme of the odd-odd nucleus ^{146}Tb, characterized by a complex structure, was extended up to about 10 MeV of excitation energy and about $30\hbar$ units of angular momentum. The spin-parity assignments for most of the observed levels have been made unambiguously by using special features of a Clover detector array. The possible configurations for the observed states have been discussed. This being a one-particle and one-hole nucleus, one expects the dominance of single-particle nature. Indeed, this is exhibited by irregular level spacings and many parallel decay branches up to spin $22\hbar$. We also observed a $\Delta J=1$ magnetic transition sequence (sequence III) which, qualitatively, appears to correspond to shears band, similar to those observed in nearby nuclei, although it may occur in multiparticle-hole excitation spectra as well. Further experimental and theoretical work is required to confirm the shears nature of this band. Experimental life time information of the levels in sequence III for reliable determination of the $B(M1)/B(E2)$ values would be particularly important to conclude about the nature of this sequence.

ACKNOWLEDGMENTS

The authors would like to thank all the participants in the joint National effort to setup the Clover array at Nuclear Science Center, New Delhi. The help received from the accelerator staff at NSC is gratefully acknowledged. The help and cooperation received from our colleagues at IUC-DAEF(CC) and NSC is appreciated. This work has been supported partially by the INDO-US, DST-NFS Grant No. (DST-NSF/RPO-017/98) and by the U.S. National Science Foundation (Grant No. INT-01115336).

[1] B. Singh, R. Zywina, and R. B. Firestone, Nucl. Data Sheets **97**, 241 (2002).
[2] T. Rzaca-Urban, Acta Phys. Pol. B **32**, 2645 (2001).
[3] R. M. Lieder *et al.*, Eur. Phys. J. A **13**, 297 (2002).
[4] Z. Marcinkowska *et al.*, Acta Phys. Pol. B **34**, 2319 (2003).
[5] M. Piiparinen *et al.*, Nucl. Phys. **A605**, 191 (1996).
[6] R. Collatz, N. Amzal, Z. Méliani, C. Schück, Ch. Vieu, J. S. Dionisio, P. Kleinheinz, and J. Blomqvist, Z. Phys. A **359** 113, (1997).
[7] Krishichayan *et al.*, *Proceedings of DAE-BRNS Symposium on Nuclear Physics, Mumbai, 2003*, edited by P. Singh and B. John, Vol. 46B, p. 144.
[8] C. Y. Xie *et al.*, Eur. Phys. J. A **19**, 7 (2004).
[9] M. Saha Sarkar *et al.*, Nucl. Instrum. Methods Phys. Res. A **491**, 113 (2002).
[10] N. S. Pattabiraman, S. N. Chintalapudi, and S. S. Ghugre, Nucl. Instrum. Methods Phys. Res. A **526**, 432, 439 (2004).
[11] D. C. Radford, Nucl. Instrum. Methods Phys. Res. A **361**, 297 (1995).
[12] N. S. Pattabiraman, S. K. Basu, S. N. Chintalapudi, U. Garg, S. S. Ghugre, S. Ray, A. K. Sinha, and S. Zhu, *Abstract of the Conference on Frontiers of Nuclear Structure, Berkeley, 2002*, LBNL-50598, p. 124.
[13] F. S. Stephens, M. A. Delenplanque, R. M. Diamond, A. O. Macchiavelli, and J. E. Draper, Phys. Rev. Lett. **54**, 2584 (1985).
[14] C. W. Beausang, D. Prévost, M. H. Bergström, G. de France, B. Haas, J. C. Lisle, Ch. Theisen, J. Timár, P. J. Twin, and J. N. Wilson, Nucl. Instrum. Methods Phys. Res. A **364**, 560 (1995).
[15] G. Duchêne, F. A. Beck, P. J. Twin, G. de France, D. Curien, L. Han, C. W. Beausang, M. A. Benteley, P. J. Nolan, and J. Simpson, Nucl. Instrum. Methods Phys. Res. A **432**, 90 (1999).
[16] Ch. Droste, K. Starosta, A. Wierzchucka, T. Morek, S. G. Rohozinskii, J. Srebrny, M. Bergstrom, B. Herskind, and E. Wesolowski, Nucl. Instrum. Methods Phys. Res. A **337**, 430 (1999).
[17] K. Starosta *et al.*, Nucl. Instrum. Methods Phys. Res. A **423**, 16 (1999).
[18] Y. Zheng *et al.*, J. Phys. G **30**, 465 (2004).
[19] R. Broda, P. J. Daly, J. H. McNeill, Z. W. Grabowski, R. V. F. Janssens, R. D. Lawson, and D. C. Radford, Z. Phys. A **334**, 11 (1989).
[20] R. Broda, Y. H. Chung, P. J. Daly, Z. W. Grabowski, J. McNeill, R. V. F. Janssens, and D. C. Radford, Z. Phys. A **316**, 125 (1984).
[21] Data extracted using the NNDC on-line Data Service from ENSDF and XUNDL databases; Y. Nagai, J. Styczen, M. Piiparinen, P. Kleinheinz, D. Bazzacco, P. von Brentano, K. O. Zell, and J. Blomqvist, Phys. Rev. Lett. **47**, 1259 (1981); K. S. Toth *et al.*, Phys. Rev. C **32**, 342 (1985); L. Esser, R. V. Jolos, and P. von Brentano, Nucl. Phys. **A650**, 157 (1999).
[22] F. R. Espinoza-Quiñones *et al.*, Phys. Rev. C **60**, 054304 (1999).
[23] M. Sferrazza, M. A. Cardona, D. Bazzacco, S. Lunardi, E. Maglione, and G. de Angelis, Z. Phys. A **354**, 157 (1996).
[24] S. Frauendorf, Rev. Mod. Phys. **73**, 463 (2001).
[25] R. M. Clark *et al.*, Nucl. Phys. **A562**, 121 (1993); G. Baldsiefen *et al.*, *ibid.* **A574**, 521 (1994); D. Mehta *et al.*, Z. Phys. A **346**, 169 (1993); A. Kuhnert *et al.*, Phys. Rev. C **46**, 133 (1992).